

^1H , ^{13}C , ^{15}N Nuclear Magnetic Resonance Backbone Assignments and Secondary Structure of Human Calcineurin B[†]

Jacob Anglister,^{*,†,§} Stephan Grzesiek,[‡] Andy C. Wang,[‡] Hao Ren,^{||} Claude B. Klee,^{||} and Ad Bax^{*,‡}

Laboratory of Chemical Physics, National Institute of Diabetes and Digestive and Kidney Diseases, and Laboratory of Biochemistry, National Cancer Institute, National Institutes of Health, Bethesda, Maryland 20892, and Department of Structural Biology, The Weizmann Institute of Science, Rehovot 76100, Israel

Received September 3, 1993; Revised Manuscript Received October 18, 1993[®]

ABSTRACT: The calmodulin- and calcium-stimulated protein phosphatase calcineurin, PP2B, consists of two subunits: calcineurin B, which binds Ca^{2+} , and calcineurin A, which contains the catalytic site and a calmodulin binding site. Heteronuclear 3D and 4D NMR experiments were carried out on a recombinant human calcineurin B which is a 170-residue protein of molecular mass 19.3 kDa, uniformly labeled with ^{15}N and ^{13}C . The nondenaturing detergent CHAPS was used to obtain a monomeric form of calcineurin B. Three-dimensional triple resonance experiments yielded complete sequential assignment of the backbone nuclei (^1H , ^{13}C , and ^{15}N). This assignment was verified by a 4D HN(COCA)NH experiment carried out with 50% randomly deuterated and uniformly ^{15}N - and ^{13}C -enriched calcineurin B. The secondary structure of calcineurin B has been determined on the basis of the $^{13}\text{C}^\alpha$ and $^{13}\text{C}^\beta$ secondary chemical shifts, $J(\text{H}^\alpha\text{H}^\beta)$ couplings, and NOE connectivities obtained from 3D ^{15}N -separated and 4D $^{13}\text{C}/^{15}\text{N}$ -separated NOESY spectra. Calcineurin B has eight helices distributed in four EF-hand, helix-loop-helix [Kretsinger, R. H. (1980) *CRC Crit. Rev. Biochem.* 8, 119–174] calcium binding domains. The secondary structure of calcineurin B is highly homologous to that of calmodulin. In comparison to calmodulin, helices B and C are shorter while helix G is considerably longer. As was observed for calmodulin in solution, calcineurin B does not have a single long central helix; rather, helices D and E are separated by a six-residue sequence in a flexible nonhelical conformation.

Calcineurin is a calmodulin- and calcium-stimulated protein phosphatase present in all eukaryotic cells, including nerve cells and T cells (Klee et al., 1987). Calcineurin consists of two tightly bound subunits, calcineurin A and calcineurin B, with molecular masses of 59 and 19.3 kDa, respectively. The presence of the two calcium-binding proteins, calcineurin B and calmodulin, is essential for the phosphatase activity of calcineurin A, and they cannot replace each other (Klee et al., 1987).

Calcineurin has been identified as the intracellular target of the immunosuppressant-immunophilin complexes FKBP-FK506¹ and cyclophilin-cyclosporin A (Liu et al., 1991, 1992; Liu, 1993a,b; Schreiber & Crabtree, 1992; Schreiber, 1992). Recent findings suggest that during T-cell activation calcineurin is a rate-limiting signal-transducing protein in Ca^{2+} -dependent pathways (Liu, 1993a): Calcineurin activity was found to parallel the exocytosis of preformed granules from cytotoxic T lymphocytes in the presence of cycloheximide, an inhibitor of transcription (Dutz et al., 1993) and it was also seen to increase IL-2 promoter activity in vivo (Clipstone & Crabtree, 1992; Liu et al., 1992). Regarding this transcription-dependent activation pathway, current evidence indicates that calcineurin, when activated by calmodulin, forwards the signal

to the nucleus by dephosphorylating the cytoplasmic subunit of NF-AT, NF-AT_c (McCaffrey et al., 1993). NF-AT_c (also known as NF-AT_p), in turn, translocates to the nucleus to join with its nuclear counterpart, NF-AT_n, and together they activate transcription of the T-cell growth factor, interleukin 2 (Flanagan et al., 1991). The translocation of NF-AT_c is prevented by cyclosporin and FK506, which exert their immunosuppressive properties, after binding to their respective immunophilins cyclophilin and FKBP, by inhibiting calcineurin, thereby preventing dephosphorylation of NF-AT_c. Cross-linking experiments between cyclophilin-cyclosporin

¹ Abbreviations: CBCA(CO)NH, three-dimensional ($^{13}\text{C}^\alpha$, $^{13}\text{C}^\beta$)- ^{15}N - ^1H spectrum correlating amide ^1H and ^{15}N with C^α and C^β shifts of the preceding residue; CBCANH, three-dimensional ($^{13}\text{C}^\alpha$, $^{13}\text{C}^\beta$)- ^{15}N - ^1H spectrum correlating amide ^1H and ^{15}N with sequential and intraresidue C^α and C^β shifts; C(CO)NH, three-dimensional ^{13}C - ^{15}N - ^1H spectrum correlating amide ^1H and ^{15}N with side-chain ^{13}C shifts of the preceding residue; CHAPS, 3-[(3-cholamidopropyl)dimethylammonio]-1-propanesulfonate; CT, constant time; FID, free induction decay; FKBP, FK506-binding protein; HBHA(CO)NH, three-dimensional ($^1\text{H}^\alpha$, $^1\text{H}^\beta$)- ^{15}N - ^1H spectrum correlating amide ^1H and ^{15}N with H^α and H^β shifts of the preceding residue; H(CCO)NH, three-dimensional ^1H - ^{15}N - ^1H spectrum correlating amide ^1H and ^{15}N with side-chain ^1H shifts of the preceding residue; HLH, helix-loop-helix; HNCA, three-dimensional ^1H - ^{15}N - $^{13}\text{C}^\alpha$ correlation; HNCO, three-dimensional ^1H - ^{15}N - $^{13}\text{C}'$ correlation; HN(COCA)NH, four-dimensional ^1H - ^{15}N - ^{15}N - ^1H spectrum correlating ^{15}N and ^1H chemical shifts of adjacent residues; HOHAHA, homonuclear Hartmann-Hahn correlation; HSQC, heteronuclear single quantum correlation; HX, hydrogen exchange; IL-2, interleukin 2; M13, 26-residue peptide comprising the skeletal muscle myosin light-chain kinase binding site for calmodulin (KRRWKKNFIAVSAANRFKKISSGAL); NF-AT, nerve factor of activated T cells; NF-AT_c, cytoplasmic subunit of NF-AT; NF-AT_n, nucleoplasmic subunit of NF-AT; NOE, nuclear Overhauser effect; NOESY, NOE spectroscopy; TPPI, time-proportional phase incrementation; 2D, 3D, and 4D, two-, three-, and four-dimensional, respectively.

[†] This work was supported by the Intramural AIDS-Directed Antiviral Program of the Office of the Director of the National Institutes of Health and by grants from the U.S.-Israel Binational Science Foundation (92-337) (J.A.) and the American Cancer Society (PF-4030) (A.C.W.).

[‡] National Institute of Diabetes and Digestive and Kidney Diseases.

[§] The Weizmann Institute of Science.

^{||} National Cancer Institute.

[®] Abstract published in *Advance ACS Abstracts*, December 1, 1993.

A or FK506-FKBP and calcineurin (both A and B subunits) suggest that the immunophilin-immunosuppressant complexes may interact primarily with the calcineurin B subunit (Li & Handschumacher, 1993).

The amino acid sequence of calcineurin B suggests the presence of four calcium binding sites of the EF-hand helix-loop-helix (HLH) type (Aitken et al., 1984). The calcium binding loops share 54% sequence identity with the calcium binding loops of calmodulin (Guerini & Klee, 1991), but outside these four calcium binding loops the degree of sequence homology is only 20%. To better understand how calcineurin B regulates the activity of calcineurin A we have initiated NMR studies of the solution structure of calcineurin B.

At the concentration required for NMR observation, the calcium-saturated form of calcineurin B dissolved in water shows resonance line widths that are indicative of aggregation (Anglister et al., 1993). The line width could be influenced to some degree by optimizing temperature, pH, and salt concentrations (Wagner, 1993), but in the absence of detergent no conditions could be found where the protein behaves as a monomeric unit. In the presence of approximately a 10-fold molar excess of the zwitterionic detergent 3-[(3-cholamidopropyl)dimethylammonio]-1-propanesulfonate (CHAPS), resonance line widths are considerably narrower and are consistent with a mass of the protein plus attached detergent of ~25 kDa. Calcineurin (the complex of calcineurin A and B) retains a high degree of activity in the presence of 20 mM CHAPS. The presence of the nondeuterated CHAPS does not interfere with the isotope-directed NMR techniques employed, as the signals from protons not attached to ^{15}N or ^{13}C are removed by isotope filtering, purge pulses, and pulsed field gradients (Anglister et al., 1993).

The present NMR study deals with genetically engineered human calcineurin B, overexpressed and isotopically enriched in *Escherichia coli* and lacking the posttranslational myristoylation of natural calcineurin B at its amino-terminal glycine residue (Aitken et al., 1982). Residues Cys¹² and Cys¹⁵⁴ were mutated to alanine and lysine, respectively, to avoid aggregation due to disulfide bond formation. These substitutions correspond to the residue types found in yeast calcineurin B.

The recent cross-linking results with FKBP and cyclophilin (Li & Handschumacher, 1993) indicate that some structural rearrangement occurs upon complexation of calcineurin B with the A subunit. Such a rearrangement is unlikely to involve large changes in secondary structure, however. The present study is therefore restricted to the secondary structure, with future work directed toward determination of the 3D structures of complexes between calcineurin B and recently identified fragments of A that bind to the B subunit.

MATERIALS AND METHODS

Molecular Cloning. Restriction enzyme digestion, ligations, DNA gel electrophoresis, and other recombinant DNA techniques were performed essentially as described by Sambrook et al. (1989). Custom oligonucleotides were synthesized on a Model 8700 DNA synthesizer (Millipore, Bedford, MA).

Mutagenesis. The coding region of human calcineurin B cDNA subcloned in the vector pBE (Guerini et al., 1989) was amplified and mutated by the polymerase chain reaction. The sense oligonucleotide, BA12 (5'-C GGG ATC CCC ATG GGA AAT GAG GCA AGT TAT CCT TTG GAA ATG GCT TCA CAC TTT GAT GCG), corresponds to the 16 amino-terminal amino acids of calcineurin B except that Cys¹² (TCG) was changed to Ala¹² (GCT). Note that the residue

numbering used in the present paper (Figure 4) starts with Met¹, although this residue was present in only a 30% fraction of the protein. A *Nco*I site was introduced in front of the initiation codon ATG and a *Bam*HI site at the 5'-end. The antisense oligonucleotide, BK154 (5'-CGC GGA TCC TCA CAC ATC TAC CAC CAT CTT TTT GTG GAT ATC TAG GCC ACC TAC AAC AGC TTT GAA TTC TTC AAA GG), is complementary to the 21 carboxyl-terminal amino acids of calcineurin B except that Cys¹⁵⁴ (TGT) was changed to Lys¹⁵⁴ (AAA). A *Bam*HI site was introduced downstream of the termination codon to facilitate subcloning. The amplified fragment was digested with *Bam*HI and ligated into the *Bam*HI site of the pBC SK(-) vector (Stratagene, La Jolla, CA) to produce pBC-BAK. The sequence of the entire coding region of the calcineurin B mutant CnB(A12K154) was verified by the method of Sanger et al. (1977). The DNA fragment containing the entire coding sequence and the termination codon was excised from pBC-BAK by digestion with *Nco*I and *Bam*HI and subcloned into the expression vector pET3d (Novagen, Madison, WI) under the control of the T7 RNA polymerase promoter (Studier et al., 1990).

Expression and Purification of Calcineurin B (A11K153). *E. coli* strain BL21 (DE3) plysS (Novagen, Madison, WI), a IDE3 lysogen containing the T7 RNA polymerase gene under the *lacUV5* promoter, was transformed with pBAKE and grown at 37 °C in M9 minimal salt medium supplemented with 0.4% glucose, 0.1 mM CaCl₂, 1 mM MgSO₄, 2 mg/L thiamin, 2 mg/L biotin, 100 mg/L ampicillin, and 30 mg/L chloramphenicol. When the absorbance at 600 nm reached 0.7, the production of protein was induced by addition of isopropyl β-D-thiogalactoside to a final concentration of 1 mM. After 5 h, the cells were harvested by centrifugation, washed, and stored at -70 °C. Calcineurin B uniformly labeled with ^{15}N and ^{13}C was obtained by growing the cells in the same medium supplemented with $^{15}\text{NH}_4\text{Cl}$ and ^{13}C D-glucose (Isotec, Miamisburg, OH) as sole nitrogen and carbon sources. M9 medium prepared with 60% D₂O/40% H₂O was used to prepare a fractionally deuterated sample of calcineurin B.

The frozen cells were routinely processed in batches corresponding to 2.5 L of original bacterial culture. The thawed cells were dispersed in 40 mL of lysis buffer (50 mM Tris-HCl, pH 8.0, 100 mM NaCl, 2 mM MgCl₂, 2 mM CaCl₂, 10 mg/L *N*-tosyl-L-phenylalanine chloromethyl ketone, 10 mg/L *N*-tosyl-L-lysine chloromethyl ketone, and 75 mg/L phenylmethanesulfonyl fluoride) and disrupted with a W-375 cell disrupter (Heat Systems, Farmingdale, NY) by 10 1-min bursts of sonication at 2-min intervals. Cell debris was removed by centrifugation at 4 °C for 1 h at 30000g. To eliminate the nucleic acids present in the supernatant fluid, its NaCl concentration was adjusted to 0.3 M prior to loading onto a DEAE-Sepharose column which had been preequilibrated with a solution containing 0.3 M NaCl, 0.1 mM CaCl₂, 50 mM Tris-HCl at pH 8, 2 mM MgCl₂, 2 μg/mL aprotinin, 1 μg/mL leupeptin, and 0.02% NaN₃. After the sample was loaded, the DEAE column was washed with this same solution and the eluent was monitored for UV absorption at 260 and 280 nm. The first fractions had the highest ratios of 280/260 absorbance; all fractions with a ratio higher than 0.5 were collected for further purification on a phenyl-Sepharose CL-4B column (Pharmacia). This column was equilibrated with a loading buffer containing 0.5 M NaCl, 0.1 mM CaCl₂, 50 mM Tris-HCl at pH 8, 2 μg/mL aprotinin, 1 μg/mL leupeptin, and 0.02% NaN₃. The DEAE fractions were adjusted to 0.5 M NaCl and loaded onto the phenyl-Sepharose column, which was washed with the loading buffer until the absorbance at

280 nm decreased to 0.1, at which point the buffer was changed to a 0.1 mM CaCl₂ solution to wash out contaminants which bind phenyl-Sepharose. When the absorbance of the eluent reached 0.01, calcineurin B was eluted with 2 mM EGTA, pH 7.5. Purity in excess of 99% was determined by polyacrylamide gel electrophoresis. The protein was concentrated using collodion bags with a molecular weight cutoff of 10 000. The calcineurin B concentration was determined by its absorbance at 276 nm using an extinction coefficient of $\epsilon^{1\%}_{276\text{nm}} = 2.41$ (Tris-HCl at pH 7.5, 0.1 M NaCl, and 1 mM CaCl₂).

Binding Experiments. The binding of the peptide M13 (KRRWKKNFIAVSAANRFKKISSGAL) to calcineurin B and calmodulin was assayed using the Hummel-Dreyer technique (1962). For this purpose we used a 1- × 30-cm column packed with Sephadex G-25 fine. The column was equilibrated with the binding buffer, 100 mM KCl, 40 mM Tris-HCl at pH 8, 0.1 mM CaCl₂, and 2 μ M M13. A 0.5-mL sample containing 20 μ M either calmodulin or calcineurin B in the running buffer was loaded onto the column and 0.4-mL fractions were monitored for absorption at 290 nm. Binding is indicated by a first peak with strong absorbance above background followed by a peak with absorbance below background (Hummel & Dreyer, 1962). It should be noted that both calmodulin and calcineurin B do not contain tryptophan and thus the contribution of M13, which has a tryptophan, to the absorption at 290 nm could be studied.

NMR Sample Preparation. Four samples were prepared for the NMR experiments. One contained 2.3 mM calcineurin B uniformly labeled (>95%) with ¹⁵N and dissolved in 95% H₂O/5% D₂O, pH 4.95, 25 mM CHAPS, and 20 mM Ca²⁺. The second sample contained 2.3 mM calcineurin B uniformly labeled (>95%) with ¹⁵N and ¹³C dissolved in the same solution. The third sample contained 1.6 mM calcineurin B uniformly labeled (>95%) with ¹⁵N and ¹³C dissolved in 99.99% D₂O at pH 4.75 (not corrected for isotope effect), 20 mM CHAPS, and 16 mM Ca²⁺. The fourth sample contained 1.4 mM calcineurin B uniformly labeled (>95%) with ¹⁵N and ¹³C and randomly ²H-labeled to ~50%, dissolved in 95% H₂O/5% D₂O at pH 5.6, 20 mM CHAPS, and 20 mM Ca²⁺.

Preparation of Calcineurin B Dissolved in D₂O. A 2-mL sample of 0.4 mM calcineurin B in H₂O solution containing 4 mM CaCl₂, 5 mM CHAPS, and 0.01% NaN₃ was lyophilized and then dissolved in 0.7 mL of D₂O. The pH was adjusted to 7.8. This sample was kept at 30 °C for 3 days to allow exchange of the amide protons and then lyophilized a second time. The solid material was dissolved in D₂O and incubated for 24 h at 30 °C. The pH was then adjusted to 4.77 and once more lyophilized and dissolved in 0.5 mL of D₂O. To identify slowly exchanging amide protons, a 2D ¹H-¹⁵N HSQC spectrum was recorded 24 h after this procedure.

NMR Spectroscopy. All NMR experiments were carried out at 37 °C on a Bruker 600-MHz AMX spectrometer equipped with an external class A/B 100-W power amplifier for the ¹³C channel. The following 3D spectra were recorded using the ¹³C/¹⁵N-labeled sample dissolved in H₂O with pulse sequences reported previously. Unless noted otherwise, a 1.5–1.8-ms scrambling pulse (instead of solvent presaturation; Messerle et al., 1989) was used at the end of the first INEPT transfer interval to suppress unwanted water and detergent magnetization. The number of complex points and acquisition times in each experiment are as follows: CT-HNCO (Grzesiek & Bax, 1992a), ¹⁵N (*F*₁) 32, 24.0 ms, ¹³CO (*F*₂) 100, 53.9 ms, ¹H ^{α} (*F*₃) 512, 55.3 ms (64 scans/hypercomplex *t*₁, *t*₂ increment); CT-HNCA (Grzesiek & Bax, 1992a), ¹⁵N (*F*₁) 32, 19.8 ms, ¹³C ^{α} (*F*₂) 53, 11.0 ms, ¹H ^{α} (*F*₃) 512, 55.3 ms

(128 scans/hypercomplex *t*₁, *t*₂ increment); HBHA(CO)NH (Grzesiek & Bax, 1993a), using a 0.79-s water presaturation pulse ($\gamma B_2/2\pi = 10$ Hz) and a 1.0-ms water scrambling pulse, ¹H ^{β} -¹H ^{α} (*F*₁) 62, 15.5 ms, ¹⁵N (*F*₂) 32, 19.8 ms, ¹H ^{α} (*F*₃) 512, 55.3 ms (128 scans/hypercomplex *t*₁, *t*₂ increment); CBCA(CO)NH (Grzesiek & Bax, 1992c), ¹³C ^{β} -¹³C ^{α} (*F*₁) 52, 6.2 ms, ¹⁵N (*F*₂) 32, 19.8 ms, ¹H ^{α} (*F*₃) 512, 55.3 ms (128 scans/hypercomplex *t*₁, *t*₂ increment); CBCANH (Grzesiek & Bax, 1992b), ¹³C ^{β} -¹³C ^{α} (*F*₁) 52, 6.2 ms, ¹⁵N (*F*₂) 32, 19.8 ms, ¹H ^{α} (*F*₃) 512, 55.3 ms (128 scans/hypercomplex *t*₁, *t*₂ increment); C(CO)NH (Grzesiek et al., 1993a), ¹³C (*F*₁) 57, 6.2 ms, ¹⁵N (*F*₂) 32, 19.8 ms, and ¹H ^{α} (*F*₃) 512, 55.3 ms (128 scans/hypercomplex *t*₁, *t*₂ increment); H(CCO)NH (Grzesiek et al., 1993a), ¹H (*F*₁) 68, 10.1 ms, ¹⁵N (*F*₂) 32, 19.8 ms, ¹H ^{α} (*F*₃) 512, 55.3 ms (128 scans/hypercomplex *t*₁, *t*₂ increment). A ¹³C/¹⁵N-separated 4D NOESY was recorded using the pulse sequence described by Kay et al. (1990) with a 60-ms mixing time, water presaturation during the delay between scans and a "soft-hard" read pulse (Sklenar & Bax, 1987) at the end of the NOESY mixing period to further suppress the H₂O resonance. The number of complex data points collected and acquisition times are ¹H (*F*₁) 40, 12.0 ms, ¹³C (*F*₂) 8, 2.7 ms, ¹⁵N (*F*₃) 16, 12.8 ms, ¹H ^{α} (*F*₄) 384, 41.4 ms (64 scans for each set of *t*₁, *t*₂, and *t*₃ values).

A 4D HN(COCA)NH experiment (Grzesiek et al., 1993b) was carried out with randomly 50% deuterated ¹⁵N/¹³C-labeled calcineurin with the following number of complex data points and acquisition times: ¹H ^{α} (*F*₁) 22, 14.5 ms, ¹⁵N (*F*₂) 20, 22.0 ms, ¹⁵N (*F*₃) 24, 26.4 ms, ¹H ^{α} (*F*₄) 512, 55.3 ms (64 scans for each set of *t*₁, *t*₂, and *t*₃ values).

The following experiments were recorded using the ¹⁵N-labeled sample: A ¹⁵N-separated 3D HOHAHA spectrum (Marion et al., 1989a) was recorded with a 35-ms mixing period using the DIPSI-2 mixing scheme (Shaka et al., 1988) and a 1.5-ms trim pulse (but no solvent presaturation) (Messerle et al., 1989) to suppress the water signal. Number of data points and acquisition times used for each dimension are ¹H (*F*₁) 100, 20.0 ms, ¹⁵N (*F*₂) 35, 26.2 ms, ¹H ^{α} (*F*₃) 512, 53.3 ms (64 scans/hypercomplex *t*₁, *t*₂ increment). The 35-ms mixing period was followed by a 17-ms NOE period (Marion et al., 1989a) to offset the positive NOE occurring during isotropic mixing. A ¹⁵N-separated 3D NOESY-HSQC was recorded using a 75-ms mixing period and presaturation of the H₂O resonance during a 0.8-s delay between the scans. A 1.5-ms trim pulse was used to further suppress the water resonance and to eliminate resonances of the detergent. The number of complex data points and acquisition times used per dimension are ¹H (*F*₁) 128, 20.5 ms, ¹⁵N (*F*₂) 40, 29.9 ms, ¹H ^{α} (*F*₃) 512, 53.3 ms (64 scans/hypercomplex *t*₁, *t*₂ increment). A 2D ¹⁵N-¹H HSQC spectrum (Bodenhausen & Ruben, 1980; Bax et al., 1990), with a 1.5-ms trim pulse (Messerle et al., 1989) at the end of the first INEPT transfer for water and detergent signal suppression, was recorded using the following number of complex data points and acquisition times: ¹⁵N (*F*₁) 256, 131.5 ms, ¹H ^{α} (*F*₂) 512, 60.4 ms (16 scans/complex *t*₁ increment). A ¹⁵N-separated HNHA spectrum (Vuister & Bax, 1993) was recorded for measuring ³J(¹H ^{α} ^{α}) couplings. The homonuclear dephasing/rephasing delay was set to 20 ms, which includes the 4.5-ms *J*_{NH} dephasing/rephasing delays. The number of complex data points and acquisition times used per dimension are ¹⁵N (*F*₁) 36, 29 ms, ¹H ^{α} (*F*₂) 52, 11.4 ms, ¹H ^{α} (*F*₃) 512, 60 ms (64 scans/hypercomplex *t*₁, *t*₂ increment). For residues Met¹-His¹⁴ and Asp¹⁶¹-Val¹⁷⁰ the *J* values derived from the resonance intensities in the HNHA spectrum were multiplied

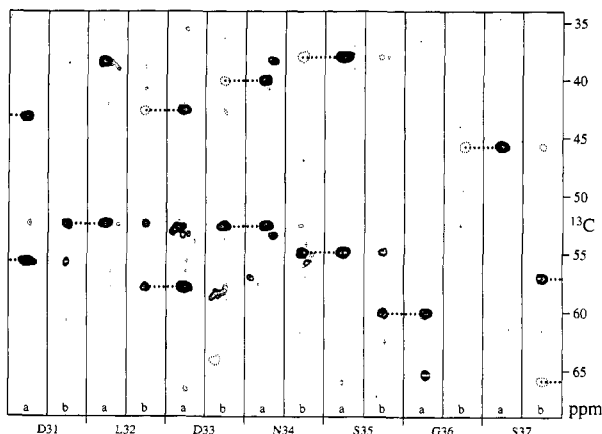


FIGURE 2: Strips of the CBCA(CO)NH (a) and CBCANH (b) spectra for the amides of residues Asp³¹–Ser³⁷ showing sequential connectivities. Resonances of negative intensity are marked by a single dashed contour.

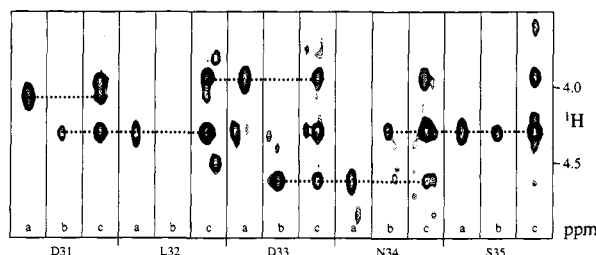


FIGURE 3: Strips of the HBHA(CO)NH (a), HOHAHA (b), and NOESY (c) spectra for the amides of residues Asp³¹–Ser³⁷ showing sequential connectivities. The resonance marked with an asterisk in panel b of Asn²⁴ results from the amide of Asn¹²³. The H^α resonance observed in panel b of Ser³⁵ nearly coincides in chemical shift with Asn²⁴-H^α.

in Figure 3, the HOHAHA, NOESY, and HBHA(CO)NH data can be used in a manner similar to the CBCANH/CBCA(CO)NH approach (Figure 2) and in practice they complement each other, particularly in cases of missing peaks or resonance degeneracy. The ¹H^N, ¹⁵N, ¹³C', ¹³C^α, ¹³C^β, ¹H^α, and ¹H^β resonance frequencies of calcineurin B are presented in Table I (supplementary material).

The ¹H, ¹³C, and ¹⁵N NMR backbone assignments were verified using a 4D HN(COCA)NH experiment, applied to ¹³C/¹⁵N-labeled calcineurin B, 50% ²H-enriched. This experiment directly correlates sequential backbone amide resonances and therefore considerably simplifies the sequential assignment procedure. Details of this experiment are described elsewhere (Grzesiek et al., 1993b). Sequential connectivities were observed for nearly all backbone amides, confirming the assignments in Table I (supplementary material).

Hydrogen–Deuterium Exchange. Slowly exchanging amide protons are indicative of hydrogen bonds. Such amide protons were identified by measuring the ¹⁵N–¹H HSQC spectrum of the D₂O sample of calcineurin B in which the amide protons were allowed to exchange with deuterium for 5 days (see Materials and Methods). The amide protons of residues Tyr⁹⁹, Asp¹⁰⁰, Asp¹⁰⁴, Tyr¹⁰⁶, Ile¹⁰⁷, Val¹¹⁵, Leu¹¹⁶, Arg¹⁴⁷, Ser¹⁴⁹, and Phe¹⁵³ (marked by filled stars in Figure 4) were found to be most resistant to deuterium exchange, with signals persisting after 5 days of incubation at elevated pH and temperature in deuterated solvent. An additional set of experiments was carried out to determine exchange of magnetization between water and amide protons (Grzesiek & Bax, 1993b). Exchange rates in the range of 0.3–100 s⁻¹ were measured for residues marked in Figure 4 by filled circles.

Fast exchanging residues are found near the amino and carboxy termini and, most interestingly, for residues Val⁸⁴–Glu⁸⁹, which are homologous with Lys⁷⁷–Glu⁸² in calmodulin. Although in the X-ray crystal structure of calmodulin these residues are in an α -helical conformation (Babu et al., 1985; Taylor et al., 1991), in solution this region is highly flexible, nonhelical, and subject to rapid hydrogen exchange (Barbato et al., 1992; Spera et al., 1991). For a number of other calcineurin B residues, NOE and ROE cross peaks to water are of opposite sign (Figure 4, open circles) (Grzesiek & Bax, 1993b). This indicates that for these amides the magnetization exchange with water is dominated by NOE/ROE effects, either to water molecules directly or to protein protons that are in rapid exchange with water (Otting et al., 1989). Most likely, NOE/ROE interactions with water for the Ser and Thr residues are mediated via the O^γ hydroxyl proton. Residues Glu⁴², Glu¹¹¹, and Glu¹⁵² occupy the 12th position in the first, third, and fourth calcium binding loops. Considering that EF-hand type calcium binding loop are all very similar in structure (Strynadka & James, 1989), it is likely that the amide protons of Glu⁴², Glu¹¹¹, and Glu¹⁵² are close in space to the O^γ protons of Ser³⁹, Ser¹⁰⁸, and Ser¹⁴⁹, respectively. All other amides for which opposite NOE and ROE values are observed are either immediately after a threonine or serine residue or adjacent to an amide proton that is in rapid exchange with water. Therefore, none of the above-mentioned NOE interactions with water provide evidence for tightly bound water molecules in calcineurin B. More precisely, the inverse of the exchange rates with bulk water for water molecules that may be present in the protein structure, and which have protons less than *ca.* 3 Å from a backbone amide, must be considerably shorter than 10 ns at the temperature where the experiments were conducted (37 °C).

Secondary Structure Determination. Secondary structure elements in proteins display distinct NOE connectivity patterns (Wüthrich, 1986). For example, α -helices are characterized by the coexistence of strong $d_{NN}(i, i + 1)$ (sequential amide proton) connectivities and $d_{\alpha N}(i, i + 3)$ connectivities (H^α of residue *i* to H^N of *i* + 3). On the other hand, β -sheets are characterized by strong $d_{\alpha N}(i, i + 1)$ signals and by the absence of the connectivities that characterize α -helices. In addition to connectivity patterns there is a very good correlation between the deviations of C^α chemical shifts from their random-coil values, i.e., secondary shifts, and the secondary structure of proteins (Spera & Bax, 1991; Wishart et al., 1991; Ikura et al., 1991; Grzesiek et al., 1992). α -Helices are characterized by positive C^α secondary shifts of *ca.* 3 ppm and C^β chemical shifts close to the random coil value, whereas β -strands are characterized by negative C^α secondary shifts and positive C^β secondary shifts. Finally, α -helical structures are characterized by small (≤ 5 Hz) H^N–H^α *J* couplings, whereas in β -sheets large (≥ 7 Hz) values are typically observed.

The $d_{NN}(i, i + 1)$, $d_{\alpha N}(i, i + 1)$, $d_{\alpha N}(i, i + 3)$, and $d_{\alpha N}(i, i + 4)$ connectivities together with the C^α and C^β secondary chemical shifts and H^N–H^α *J* coupling data are presented in Figure 4. The precise values of H^N–H^α *J* couplings are listed in Table I (supplementary material). The data in Figure 4 identify the location of eight helices and four short β -strands. The helices span the regions (A) Ala¹⁷–Leu³⁰, (B) Val⁴⁰–Ser⁴⁵, (C) Val⁵⁵–Phe⁶², (D) Phe⁷²–Gln⁸¹, (E) Lys⁸⁸–Tyr⁹⁹, (F) Asn¹⁰⁹–Met¹¹⁹, (G) Asp¹²⁶–Ala¹⁴⁰, and (H) Phe¹⁵⁰–Gly¹⁵⁸. Except for helix C, the beginnings of the helices are marked by a strong C^α secondary shift following a sequence of at least two residues with small or negative C^α secondary shifts; the ends of all eight helices are marked by negative or

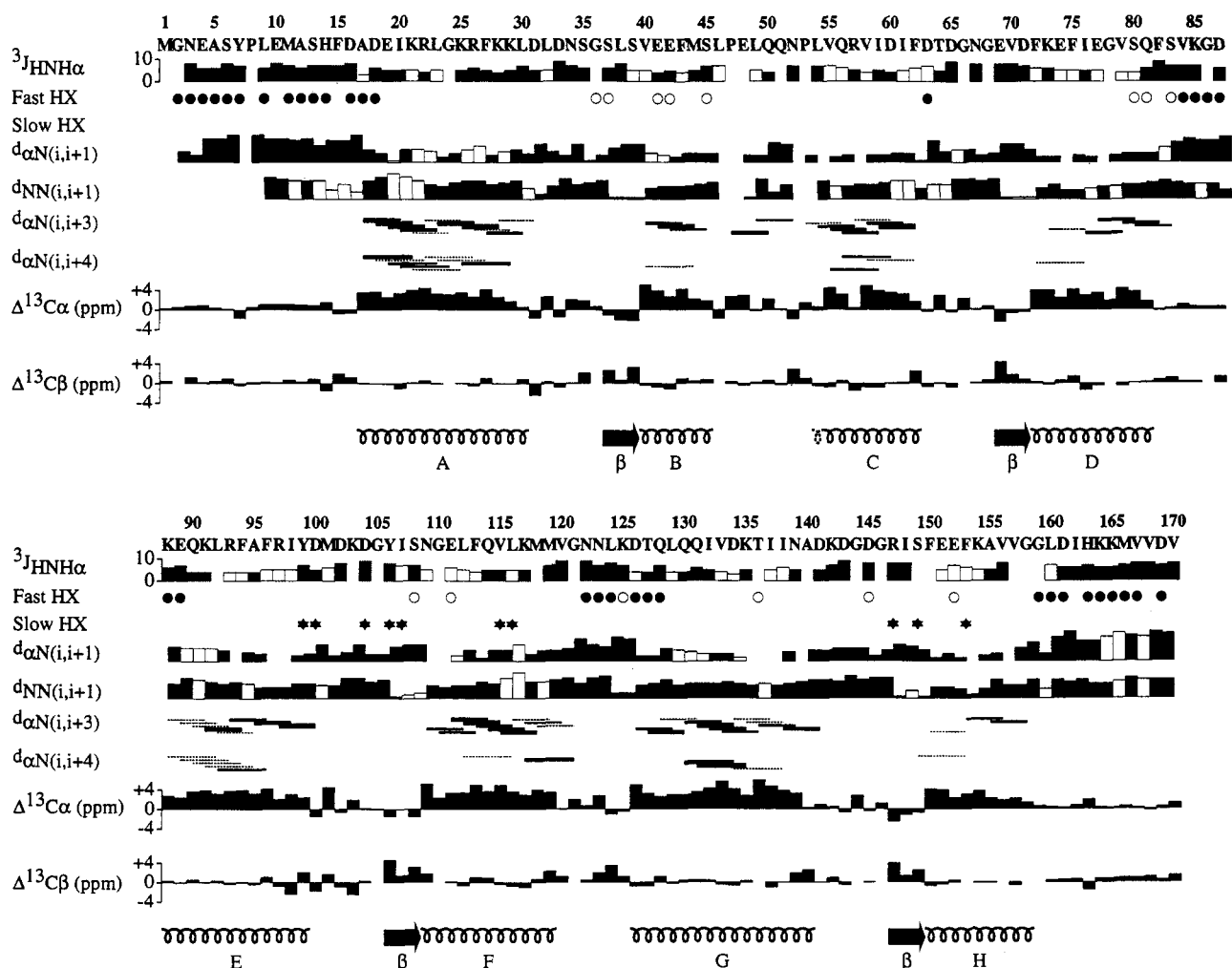


FIGURE 4: Summary of the calcineurin B data on sequential and medium-range NOEs involving the H^N and H^α protons, amide exchange data, $J(H^N H^\alpha)$ couplings, and $^{13}C^\alpha$ and $^{13}C^\beta$ secondary shifts ($\Delta^{13}C^\alpha$ and $\Delta^{13}C^\beta$) observed for calcineurin B, together with the secondary structure deduced from these data. For the $^3J(H^N H^\alpha)$ data, open boxes refer to upper limits for the J coupling, based on a cross-peak intensity in the HNHA spectrum that is below the signal-to-noise threshold. Shaded boxes refer to amides for which the H^N - ^{15}N correlation is partially overlapping, resulting in a less precise measurement of $J(H^N H^\alpha)$. J values for glycine residues are reported in the supplementary material only. Residues with amide protons subject to fast ($> \sim 0.3 \text{ s}^{-1}$) hydrogen exchange (HX) are marked by filled circles. Amide protons which exchange magnetization with water via an (indirect) NOE effect are marked by open circles. Amide protons subject to extremely slow hydrogen exchange are marked by filled stars. NOE connectivities that could not be established unambiguously because of overlap are marked by open boxes ($d_{\alpha N}$ and d_{NN}) or dashed lines ($d_{\alpha N}$).

very small C^α secondary shifts, increases in $J(H^N H^\alpha)$ values, and the absence of $d_{\alpha N}(i, i + 3)$ connectivities. Except for Arg⁵⁷, which displays a small positive C^α secondary shift, all residues within the helices indeed exhibit strong positive C^α secondary shifts and small $J(H^N H^\alpha)$ couplings. Also, strong $d_{NN}(i, i + 1)$ connectivities are observed together with numerous $d_{\alpha N}(i, i + 3)$ and several weak $d_{\alpha N}(i, i + 4)$ connectivities. The latter type of connectivity is only expected in α -helices (Wüthrich, 1986).

Ca²⁺ Binding Loops. Each calcium binding site consists of 12 residues and is flanked by two α -helices, forming a HLH EF-hand motif. There are four Ca²⁺ binding sites in calcineurin B, each made of a six-residue loop (Asp³¹-Gly³⁶, Asp⁶³-Gly⁶⁸, Asp¹⁰⁰-Gly¹⁰⁵, and Asp¹⁴¹-Gly¹⁴⁶) followed by three residues in a β -sheet conformation (Ser³⁷-Ser³⁹, Glu⁶⁹-Asp⁷¹, Tyr¹⁰⁶-Ser¹⁰⁸, and Arg¹⁴⁷-Ser¹⁴⁹), which are in turn followed by three residues which form the beginning of the successive helix (Val⁴⁰-Glu⁴², Phe⁷²-Glu⁷⁴, Asn¹⁰⁹-Glu¹¹¹, and Phe¹⁵⁰-Glu¹⁵²). The boundaries of a β -strand are more easily determined on the basis of strong $d_{\alpha N}(i, i + 1)$ and weak or absent $d_{NN}(i, i + 1)$ connectivities and negative C^α and positive C^β secondary shifts. Long-range NOEs between the backbone

protons on different strands are needed to establish which strand is adjacent to which other strand and to determine whether the β -sheet is parallel or antiparallel. The ^{15}N -separated 3D NOESY-HSQC reveals medium-intensity NOE connectivities between the amide protons of Leu³⁸ and Val⁷⁰ and between Ile¹⁰⁷ and Ile¹⁴⁸, while the $^{13}C/^{15}N$ -separated 4D NOESY reveals weak NOE connectivities between the amide proton of Ile¹⁴⁸ and H^α of Ser¹⁰⁸ and between the amide proton of Leu³⁸ and the H^α of Asp⁷¹. These NOE connectivities indicate that strand Ser³⁷-Ser³⁹ forms an antiparallel sheet with Phe⁷²-Glu⁷⁴, whereas Asn¹⁰⁹-Glu¹¹¹ forms an antiparallel sheet with Phe¹⁵⁰-Glu¹⁵². This pairing of the β -strands is similar to that observed in calmodulin (Babu et al., 1988).

Connecting Loops. Calcineurin B contains two other loops (Leu⁴⁶-Pro⁵³ and Val¹²⁰-Lys¹²⁵) which connect the first and second EF-hand in each of the protein's two domains. None of the amide protons of residues Leu⁴⁶-Gln⁵¹ in the first loop are in fast exchange with solvent; for the last residues in this loop, Asn⁵² and Leu⁵⁴, the absence of exchange cannot be established unambiguously because of resonance overlap. Strong positive secondary shifts for the C^α of three residues within this loop (Pro⁴⁷, Glu⁴⁸, and Gln⁵⁰) are observed, together

with weak $d_{\alpha N}(i, i + 1)$ connectivities for Glu⁴⁸–Gln⁵⁰ and two $d_{\alpha N}(i, i + 3)$ connectivities. This suggests the possible presence of multiple turns. However, the current data do not allow a more precise characterization of the structure of this loop. The second loop is shorter and presumably more extended, based on the presence of strong $d_{\alpha N}(i, i + 1)$ connectivities and large $J(\text{H}^N\text{H}^\alpha)$ values. Rapid hydrogen exchange is observed for three residues in this loop and for the first three residues of helix G, following this loop (Grzesiek and Bax, 1993b).

Flexible Segments. Rapid amide hydrogen exchange, relatively narrow resonances, near random coil chemical shifts, strong $d_{\alpha N}(i, i + 1)$ connectivities, and most importantly, the absence of intermediate-range ($i, i + 3$) and ($i, i + 4$) NOE connectivities are observed for three regions: the amino terminus (Met¹–Asp¹⁶), the carboxy terminus (Gly¹⁵⁹–Val¹⁷⁰), and the linker between helix D and E (Phe⁸²–Asp⁸⁷). These data suggest that these three regions are subject to rapid conformational exchange.

DISCUSSION

The data presented above provide the first experimental evidence that calcineurin B is highly homologous in its secondary structure to calmodulin. The four calcium binding sites of this protein display the typical EF-hand conformation characterized by a helix–loop–helix motif. The calcium binding loops of calcineurin B are highly homologous to those of calmodulin. They all contain the invariant aspartate, glycine, and glutamate residues at loop positions 1, 6, and 12, respectively, and follow the consensus sequence for Ca²⁺ binding sites (Szebenyi & Moffat, 1986; Strynadka & James, 1989). In all four calcium binding sites the second helix begins at position 10 of the calcium binding loop, immediately following the three-residue β -strand. The helices preceding and following the calcium binding sites vary in length from 6 to 15 residues. Helix B (Val⁴⁰–Ser⁴⁵), the shortest of these, is four residues shorter than the corresponding helix in calmodulin, presumably due to the presence of a Pro in position 47 of calcineurin B. Helix C (Leu⁵⁴– or Val⁵⁵–Phe⁶²) is also several residues shorter than helix C of calmodulin, which may be attributed to the absence of three codons in the gene of calcineurin B as compared to the calmodulin gene. Conversely, helix G of calcineurin is four residues longer than the corresponding helix in calmodulin, which corresponds to four additional amino acids in the calcineurin sequence relative to that of calmodulin. These differences in the lengths of the helices may have implications on the interaction of calcineurin A with calcineurin B (and with calmodulin). Other differences are observed in the regions connecting helices B and C and helices F and G. In calmodulin, these loops were found to be flexible and subject to rapid hydrogen exchange (Barbato et al., 1992; Spera et al., 1991). In contrast, the connecting region between helices B and C in calcineurin B does not exhibit rapid hydrogen exchange. Many of the residues in the loop connecting helices F and G exchange rapidly with solvent. In contrast to calmodulin, significant secondary C α shifts are found for residues in these two regions of calcineurin B, suggesting that they adopt a well-ordered conformation. In addition to these differences, calcineurin B has 9 and 10 additional residues relative to calmodulin at the amino and carboxy termini, respectively. The importance of the N-terminus of calcineurin B is implicated by the fact that although myristoylation of the N-terminal glycine increases the affinity of calcineurin B for calcineurin A only 3-fold, it is essential for the phosphatase activity of calcineurin (Ren & Klee, 1993).

Although our present results for free calcineurin B indicate that the N-terminal residues of calcineurin B are disordered, it is likely that this region in myristoylated calcineurin B adopts a well-defined structure upon interaction with calcineurin A. However, considering that the genetically engineered non-myristoylated form of calcineurin B, used in our study, retains very tight binding to the A subunit, it is unlikely that myristoylation has significant effects on the structure in other regions of the B subunit.

NOE interactions between the β -strands of calcium binding loops I and II and, similarly, calcium loops III and IV indicate that the first and second EF-hands and, similarly, the third and fourth EF-hands form small globular domains, each containing two calcium binding sites. These globular domains are connected by helix D, a flexible connection region (Val⁸⁴–Lys⁸⁸), and helix E. The NMR characteristics of the connection region are similar to those observed in the solution structure of calmodulin (Ikura et al., 1991; Barbato et al., 1992), where a flexible stretch of six residues disrupts the 27-residue α -helix observed in the crystalline state (Babu et al., 1985; Taylor et al., 1991). However, at the present time it is not clear whether the two domains of calcineurin B are connected by a flexible linker, as observed for free calmodulin in solution (Barbato et al., 1992), or whether the two domains interact to form a globular structure similar to that of calmodulin when it is complexed with its target peptides (Ikura et al., 1992; Meador et al., 1992).

The differences in structure between calcineurin B and calmodulin manifest themselves in several other properties: First, while calmodulin tightly binds M13, no significant binding of M13 to calcineurin B was observed at 2 μM concentration of M13 (data not shown). Second, calcineurin B, at concentrations up to 10⁻⁶ M, neither activates the phosphatase activity of calcineurin A (3 \times 10⁻⁸ M) nor inhibits its stimulation by 3 \times 10⁻⁸ M calmodulin; calcineurin B was also unable to reverse the inhibition of calmodulin stimulation by 6 \times 10⁻⁸ M of the M13 peptide. Third, unlike calmodulin, calcineurin B aggregates in solution and monomeric molecules suitable for NMR studies could be obtained only in the presence of the detergent CHAPS. This suggests the presence of exposed hydrophobic surfaces which promote aggregation of the protein. Recently, a 28 amino acid peptide from calcineurin A has been identified which binds calcineurin B with a dissociation constant of 3 μM (P. Stemmer, M. H., Krinks, and C. B. Klee, manuscript in preparation). Our further structural studies of calcineurin are aimed at addressing the mode of interaction between calcineurin B and calcineurin A and at comparing this interaction to that observed in complexes of calmodulin with its peptide ligands.

ACKNOWLEDGMENT

We thank Geerten Vuister for assistance with measurement of the $J(\text{H}^N\text{H}^\alpha)$ coupling constants, Dan Garrett and Frank Delaglio for developing the software used to process and analyze the NMR data, Rolf Tschudin for the development of spectrometer hardware, Daniel Feigelson for careful reading of the manuscript, and Juanita Eldridge for the synthesis of oligonucleotides.

SUPPLEMENTARY MATERIAL AVAILABLE

One table containing the H^N, H α , H β , ¹⁵N, ¹³CO, ¹³C α , and ¹³C β chemical shifts and ³ $J(\text{H}^N\text{H}^\alpha)$ coupling constant data (8 pages). Ordering information is given on any current masthead page.

REFERENCES

- Aitken, A., Cohen, P., Snatikarn, S., Williams, D. H., Calder, A. G., & Klee, C. B. (1982) *FEBS Lett.* 150, 314–317.
- Aitken, A., Klee, C. B., & Cohen, P. (1984) *Eur. J. Biochem.* 139, 663–671.
- Anglister, J., Grzesiek, S., Ren, J., Klee, C. B., & Bax, A. (1993) *J. Biomol. NMR* 3, 121–126.
- Babu, Y. S., Sack, J. S., Greenhough, T. J., Bugg, C. E., Means, A. R., & Cook, W. J. (1985) *Nature* 315, 37–40.
- Babu, Y. S., Bugg, C. E., & Cook, W. J. (1988) *J. Mol. Biol.* 204, 191–204.
- Barbato, G., Ikura, M., Kay, L. E., Pastor, R. W., & Bax, A. (1992) *Biochemistry* 31, 5269–5278.
- Bax, A., Ikura, M., Kay, L. E., Torchia, D. A., & Tschudin, R. (1990) *J. Magn. Reson.* 86, 304–318.
- Bodenhausen, G., & Ruben, D. J. (1980) *Chem. Phys. Lett.* 69, 185–188.
- Clipstone, N. A., & Crabtree, G. R. (1992) *Nature* 357, 695–697.
- Clore, G. M., & Gronenborn, A. M. (1989) *CRC Crit. Rev. Biochem. Mol. Biol.* 24, 479–564.
- Dutz, J. P., Fruman, D. A., Burakoff, S. J., & Bierer, B. E. (1993) *J. Immunol.* 150, 2591–2598.
- Flanagan, W. M., Corthesy, B., Bram, R. J., & Crabtree, G. R. (1991) *Nature* 352, 803–807.
- Garrett, D. S., Powers, R., Gronenborn, A. M., & Clore, G. M. (1991) *J. Magn. Reson.* 95, 214–220.
- Grzesiek, S., & Bax, A. (1992a) *J. Magn. Reson.* 96, 432–440.
- Grzesiek, S., & Bax, A. (1992b) *J. Magn. Reson.* 99, 201–207.
- Grzesiek, S., & Bax, A. (1992c) *J. Amer. Chem. Soc.* 114, 6291–6293.
- Grzesiek, S., & Bax, A. (1993a) *J. Biomol. NMR* 3, 185–204.
- Grzesiek, S., & Bax, A. (1993b) *J. Biomol. NMR* 3, 627–638.
- Grzesiek, S., Döbeli, H., Gentz, R., Garotta, G., Labhardt, A. M., & Bax, A. (1992) *Biochemistry* 31, 8180–8190.
- Grzesiek, S., Anglister, J., & Bax, A. (1993a) *J. Magn. Reson.* 101, Series B, 114–119.
- Grzesiek, S., Anglister, J., Ren, H., & Bax, A. (1993b) *J. Am. Chem. Soc.* 115, 4369–4370.
- Guerini, D., & Klee, C. B. (1991) *Adv. Protein Phosphatases* 6, 391–410.
- Guerini, D., Krinks, M. H., Sikela, J. M., Hahn, W. E., & Klee, C. B. (1989) *DNA* 8, 675–682.
- Hummel, J. P., & Dreyer, W. J. (1962) *Biochem. Biophys. Acta* 63, 530–532.
- Ikura, M., Spera, S., Barbato, G., Kay, L. E., Krinks, M., & Bax, A. (1991) *Biochemistry* 30, 9217–9227.
- Ikura, M., Clore, G. M., Gronenborn, A. M., Zhu, G., Klee, C. B., & Bax, A. (1992) *Science* 256, 632–638.
- Kay, L. E., Clore G. M., Bax, A., & Gronenborn, A. M. (1990) *Science* 249, 411–414.
- Klee, C. B., Draetta, G., & Hubbard, M. (1987) *Adv. Enzymol. Relat. Areas Mol. Biol.* 61, 149–200.
- Kretsinger, R. H. (1980) *CRC Crit. Rev. Biochem.* 8, 119–174.
- Li, W., & Handschumacher, R. E. (1983) *J. Biol. Chem.* 268, 14040–14044.
- Liu, J. (1993a) *Immunol. Today* 14, 290–295.
- Liu, J. (1993b) *Trends Pharmacol. Sci.* 14, 182–188.
- Liu, J., Farmer, J. D., Jr., Lane, W. S., Friedman, J., Weissman, I., & Schreiber, S. L. (1991) *Cell* 66, 807–815.
- Liu, J., Albers, M. W., Wandless, T. J., Luan, S., Alber, D. G., Belshaw, P. J., Cohen, P., MacKintosh, C., Klee, C. B., & Schreiber, S. L. (1992) *Biochemistry* 31, 3896–3901.
- Logan, T. M., Olejniczak, E. T., Xu, R. X., & Fesik, S. W. (1992) *FEBS Lett.* 314, 413–418.
- Marion, D., Driscoll, P. C., Kay, L. E., Wingfield, P. T., Bax, A., Gronenborn, A. M., & Clore, G. M. (1989a) *Biochemistry* 28, 6510–6156.
- Marion, D., Ikura, M., Tschudin, R., & Bax, A. (1989b) *J. Magn. Reson.* 85, 393–399.
- McCaffrey, P. G., Perrino, B. A., Soderling, T. R., & Rao, A. (1993) *J. Biol. Chem.* 268, 3747–3752.
- Meador, W. E., Means, A. R., & Quioco, F. A. (1992) *Science* 257, 1251–1255.
- Messerle, B. A., Wider, G., Otting, G., Weber, C., & Wüthrich, K. (1989) *J. Magn. Reson.* 85, 608–613.
- Montelione, G. T., Lyons, B. A., Emerson, S. D., & Tashiro, M. (1992) *J. Am. Chem. Soc.* 114, 10974–10975.
- Otting, G., & Wüthrich, K. (1989) *J. Am. Chem. Soc.*, 111, 1871–1875.
- Ren, H., & Klee, C. B. (1993) *Seventh Symposium of the Protein Society*, Abstract 389–T.
- Sambrook, J., Fritsch, E. F., & Maniatis, T. (1989) *Molecular Cloning: A Laboratory Manual*, 2nd ed., Cold Spring Harbor Laboratory, Cold Spring Harbor, NY.
- Sanger, F., Nicklen, S., & Coulson, A. R. (1977) *Proc. Natl. Acad. Sci. U.S.A.* 74, 5463–5467.
- Schreiber, S. L. (1992) *Cell* 70, 365–368.
- Schreiber, S. L., & Crabtree, G. R. (1992) *Immunol. Today* 13, 136–142.
- Shaka, A. J., Lee, C. J., & Pines, A. (1988) *J. Magn. Reson.* 77, 274–293.
- Sklenar, V., & Bax, A. (1987) *J. Magn. Reson.* 74, 469–479.
- Spera, S., & Bax, A. (1991) *J. Am. Chem. Soc.* 113, 5490–5492.
- Spera, S., Ikura, M., & Bax, A. (1991) *J. Biomol. NMR* 1, 155–165.
- Strynadka, N. C. J., & James, M. N. G. (1989) *Annu. Rev. Biochem.* 58, 951–998.
- Studier, F. W., Rosenberg, A. H., Dunn, J. J., & Dubendorff, J. W. (1990) *Methods Enzymol.* 185, 60–89.
- Szebenyi, D. M. E., & Moffat, K. (1986) *J. Biol. Chem.* 261, 8761–8777.
- Taylor, D. A., Sack, J. S., Maune, J. F., Beckingham, K., & Quioco, F. A. (1991) *J. Biol. Chem.* 266, 21375–21380.
- Vuister, G. W., & Bax, A. (1993) *J. Am. Chem. Soc.* 115, 7772–7777.
- Wagner, G. (1993) *J. Biomol. NMR* 3, 375–385.
- Wishart, D. S., Sykes, B. D., & Richards, F. M. (1991) *J. Mol. Biol.* 222, 311–333.
- Wüthrich, K. (1986) *NMR of Proteins and Nucleic Acids*, Wiley, New York.